- Hydrogels Composed of Organic Amphiphiles and α-Cyclodextrin: Supramolecular Networks of Their Pseudorotaxanes in Aqueous Media
  Taira, T.; Suzaki, Y.; Osakada, K. *Chem. Eur. J.* **2010**, *16*, 6518-6529.
  Abstract:

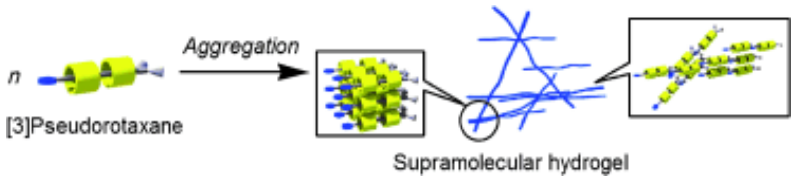


Mixtures of *N*-alkyl pyridinium compounds [py-*N*-$(CH_2)_n OC_6H_3$-3,5-$(OMe)_2$]$^+$($X^-$) (**1b**Cl: *n*=10, X=Cl; **1c**Br: *n*=12, X=Br) and α-cyclodextrin (α-CD) form supramolecular hydrogels in aqueous media. The concentrations of the two components influences the sol-gel transition temperature, which ranges from 7 to 67 ºC. Washing the hydrogel with acetone or evaporation of water left the xerogel, and $^{13}C$ CP/MAS NMR measurements, powder X-ray diffraction (XRD), and scanning electron microscopy (SEM) revealed that the xerogel of **1b**Cl (or **1c**Br) and α-CD was composed of pseudorotaxanes with high crystallinity. $^{13}C\{^1H\}$ and $^1H$ NMR spectra of the gel revealed the detailed composition of the components. The gel from **1b**Cl and α-CD contains the corresponding [2]- and [3]pseudorotaxanes, [**1b**·(α-CD)]Br and [**1b**·$(\alpha\text{-CD})_2$]Br, while that from **1c**Br and α-CD consists mainly of [3]pseudorotaxane [**1c**·$(\alpha\text{-CD})_2$]Br. 2D ROESY $^1H$ NMR measurements suggested intermolecular contact of 3,5-dimethoxyphenyl and pyridyl end groups of the axle component. The presence of the [3]pseudorotaxane is indispensable for gel formation. Thus, intermolecular interaction between the end groups of the axle component and that between α-CDs of the [3]pseudorotaxane contribute to formation of the network. The supramolecular gels were transformed into sols by adding denaturing agents such as urea, $C_6H_3$-1,3,5-$(OH)_3$, and [py-*N*-*n*Bu]$^+$($Cl^-$).

- Ligand-to-Ligand Charge-Transfer Transitions of Platinum(II) Complexes with Arylacetylide Ligands with Different Chain Lengths: Spectroscopic Characterization, Effect of Molecular Conformations, and Density Functional Theory Calculations
  Ming Tong, G. S.; Law, Y.-C.; Kui, S. C. F.; Zhu, N.; Leung, K. H.; Phillips, D. L.; Che, C.-M. *Chem. Eur. J.* **2010**, *16*, 6540-6554.
  Abstract:

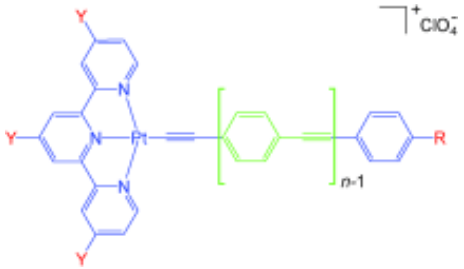


The complexes [Pt(*t*$Bu_3$tpy){C≡C$(C_6H_4C\equiv C)_{n-1}$R}]$^+$ (*n*=1: R=alkyl and aryl (Ar); *n*=1-3: R=phenyl (Ph) or Ph-$N(CH_3)_2$-4; *n*=1 and 2, R=Ph-$NH_2$-4; *t*$Bu_3$tpy=4,4′,4″-tri-*tert*-butyl-2,2′:6′,2″-terpyridine) and [Pt($Cl_3$tpy)(C≡CR)]$^+$ (R=*tert*-butyl (*t*Bu), Ph, 9,9′-dibutylfluorene, 9,9′-dibutyl-7-dimethyl-amine-fluorene; $Cl_3$tpy=4,4′,4″-trichloro-2,2′:6′,2″-terpyridine) were prepared. The effects of substituent(s) on the terpyridine (tpy) and acetylide ligands and chain length of arylacetylide ligands on the absorption and emission spectra were examined. Resonance Raman (RR) spectra of [Pt(*t*$Bu_3$tpy)(C≡CR)]$^+$ (R=*n*-butyl, Ph, and $C_6H_4$-$OCH_3$-4) obtained in acetonitrile at 298 K reveal that the structural distortion of the C≡C bond in the electronic excited state obtained by 502.9 nm

excitation is substantially larger than that obtained by 416 nm excitation. Density functional theory (DFT) and time-dependent DFT (TDDFT) calculations on $[Pt(H_3tpy)(C{\equiv}CR)]^+$ (R= *n*-propyl (*n*Pr), 2-pyridyl (Py)), $[Pt(H_3tpy)\{C{\equiv}C(C_6H_4C{\equiv}C)_{n\text{-}1}Ph\}]^+$ (*n*=1-3), and $[Pt(H_3tpy)\{C{\equiv}C(C_6H_4C{\equiv}C)_{n\text{-}1}C_6H_4\text{-}N(CH_3)_2\text{-}4\}]^+/+H^+$ (*n*=1-3; $H_3$tpy=non-substituted terpyridine) at two different conformations were performed, namely, with the phenyl rings of the arylacetylide ligands coplanar ("cop") with and perpendicular ("per") to the $H_3$tpy ligand. Combining the experimental data and calculated results, the two lowest energy absorption peak maxima, $\lambda_1$ and $\lambda_2$, of $[Pt(Y_3tpy)(C{\equiv}CR)]^+$ (Y=*t*Bu or Cl, R=aryl) are attributed to $^1[\pi(C{\equiv}CR){\rightarrow}\pi^*(Y_3tpy)]$ in the "cop" conformation and mixed $^1[d_\pi(Pt){\rightarrow}\pi^*(Y_3tpy)]/^1[\pi(C{\equiv}CR){\rightarrow}\pi^*(Y_3tpy)]$ transitions in the "per" conformation. The lowest energy absorption peak $\lambda_1$ for $[Pt(tBu_3tpy)\{C{\equiv}C(C_6H_4C{\equiv}C)_{n\text{-}1}C_6H_4\text{-}H\text{-}4\}]^+$ (*n*=1-3) shows a redshift with increasing chain length. However, for $[Pt(tBu_3tpy)\{C{\equiv}C(C6H4C{\equiv}C)_{n\text{-}1}C_6H_4\text{-}N(CH_3)_2\text{-}4\}]^+$ (*n*=1-3), $\lambda_1$ shows a blueshift with increasing chain length *n*, but shows a redshift after the addition of acid. The emissions of $[Pt(Y_3tpy)(C{\equiv}CR)]^+$ (Y=*t*Bu or Cl) at 524-642 nm measured in dichloromethane at 298 K are assigned to the $^3[\pi(C{\equiv}CAr){\rightarrow}\pi^*(Y_3tpy)]$ excited states and mixed $^3[d_\pi(Pt){\rightarrow}\pi^*(Y_3tpy)]/^3[\pi(C{\equiv}C){\rightarrow}\pi^*(Y_3tpy)]$ excited states for R=aryl and alkyl groups, respectively. $[Pt(tBu_3tpy)\{C{\equiv}C(C_6H_4C{\equiv}C)_{n\text{-}1}C_6H_4\text{-}N(CH_3)_2\text{-}4\}]^+$ (*n*=1 and 2) are nonemissive, and this is attributed to the small energy gap between the singlet ground state ($S_0$) and the lowest triplet excited state ($T_1$).

- Gelation Grow with the flow
  Pasquali, M. *Nature materials* **2010**, *9*, 381-382.
  Abstract:

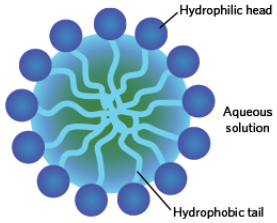


**Figure 1 |** A schematic of a spherical micelle of surfactant molecules in aqueous solution. The hydrophobic sections of the surfactant are close to each other and the hydrophilic head groups face outwards into the solution.

So far, flow-induced transitions and structures formed by the assembly of surfactant micelles have been reversible. Now, a microporous extensional flow process forms a permanent gel, which remains intact even after flow has stopped. oap has been used since the earliest recorded history. However, its active ingredient — surfactant molecules — was not termed as such until the 1950s. Since this time, the science of surfactants has been studied intensely because of fundamental interest and because of their widespread use in high-value applications such as detergents, personal care products, pharmaceuticals and oil recovery. Despite this extensive and productive history, the surfactant molecule still manages to surprise us.

- The thermodynamic origin of hysteresis in insertion batteries
  Dreyer, W.; Jamnik, J.; Guhlke, C.; Huth, R.; Moškon, J.; Gaberšcek, M. *Nature materials* **2010**, *9*, 448-453.
  Abstract:

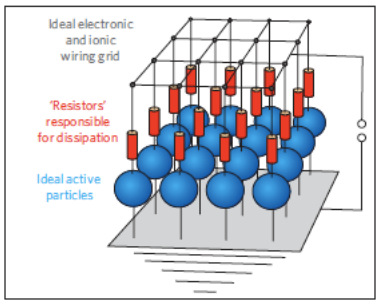


Lithium batteries are considered the key storage devices for most emerging green technologies such as wind and solar technologies or hybrid and plug-in electric vehicles. Despite the tremendous recent advances in battery research, surprisingly, several fundamental issues of increasing practical importance have not been adequately tackled. One such issue concerns the energy efficiency. Generally, charging of 1010–1017 electrode particles constituting a modern battery electrode proceeds at (much) higher voltages than discharging. Most importantly, the hysteresis between the charge and discharge voltage seems not to disappear as the charging/discharging current vanishes. Herein we present, for the first time, a general explanation of the occurrence of inherent hysteretic behaviour in insertion storage systems containing multiple particles. In a broader sense, the model also predicts the existence of apparent equilibria in battery electrodes, the sequential particle-by-particle charging/discharging mechanism and the disappearance of two-phase behaviour at special experimental conditions.

- The key nickel enzyme of methanogenesis catalyses the anaerobic oxidation of methane
  Scheller, S.; Goenrich, M.; Boecher, R.; Thauer, R. K.; Jaun, B. *Nature* **2010**, *465*, 606–608.
  Abstract:

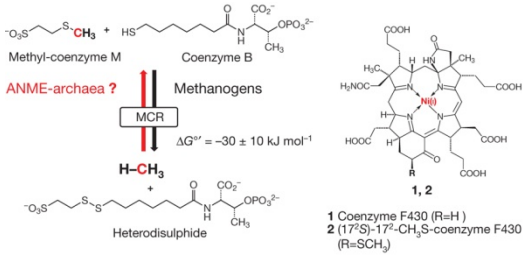


Large amounts (estimates range from 70 Tg per year to 300 Tg per year) of the potent greenhouse gas methane are oxidized to carbon dioxide in marine sediments by communities of methanotrophic archaea and sulphate-reducing bacteria1, and thus are prevented from escaping into the atmosphere. Indirect evidence indicates that the anaerobic oxidation of methane might proceed as the reverse of archaeal methanogenesis from carbon dioxide with the nickel-containing methyl-coenzyme M reductase (MCR) as the methane-activating enzyme. However, experiments showing that MCR can catalyse the endergonic back reaction have been lacking. Here we report that purified MCR from Methanothermobacter marburgensis converts methane into methyl-coenzyme M under equilibrium conditions with apparent Vmax (maximum rate) and Km (Michaelis constant) values consistent with the observed in vivo kinetics of the anaerobic oxidation of methane with sulphate. This result supports the hypothesis of 'reverse methanogenesis' and is paramount to understanding the still-unknown mechanism of the last step of methanogenesis. The ability of MCR to cleave the particularly strong C–H bond of methane without the involvement of highly reactive oxygen-derived intermediates is directly relevant to catalytic C–H activation, currently an area of great interest in chemistry.

- The folding cooperativity of a protein is controlled by its chain topology
  Shank, E. A.; Cecconi, C.; Dill, J. W.; Marqusee, S.; Bustamante, C. *Nature* **2010**, *465*, 637–640.
  Abstract:

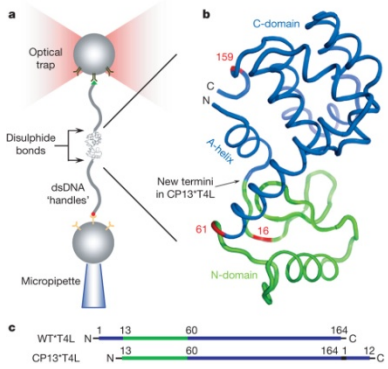


The three-dimensional structures of proteins often show a modular architecture comprised of discrete structural regions or domains. Cooperative communication between these regions is important for catalysis, regulation and efficient folding; lack of coupling has been implicated in the formation of fibrils and other misfolding pathologies. How different structural regions of a protein communicate and contribute to a protein's overall energetics and folding, however, is still poorly understood. Here we use a single-molecule optical tweezers approach to induce the selective unfolding of particular regions of T4 lysozyme and monitor the effect on other regions not directly acted on by force. We investigate how the topological organization of a protein (the order of structural elements along the sequence) affects the coupling and folding cooperativity between its domains. To probe the status of the regions not directly subjected to force, we determine the free energy changes during mechanical unfolding using Crooks' fluctuation theorem. We pull on topological variants (circular permutants) and find that the topological organization of the polypeptide chain critically determines the folding cooperativity between domains and thus what parts of the folding/unfolding landscape are explored. We speculate that proteins may have evolved to select certain topologies that increase coupling between regions to avoid areas of the landscape that lead to kinetic trapping and misfolding.

- Conversion of carbonyl compounds to alkynes: general overview and recent developments
  Habrant, D.; Rauhala, V.; Koskinen, A. M. P. *Chem. Soc. Rev.* **2010**, *39*, 2007 – 2017.
  Abstract:

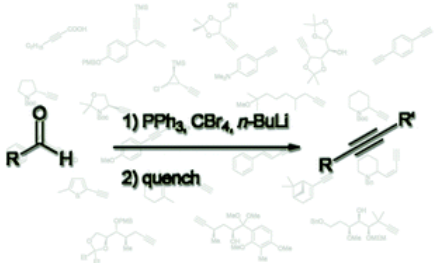


The preparation of alkynes from carbonyl compounds *via* a one-carbon homologation has become a very useful pathway for the synthesis of acetylenic compounds, both internal and terminal. This *tutorial review* provides an overview of the different methods available for this transformation, including their scope and limitations, recent developments and applications in total syntheses.

- Fluorescent chemosensors for $Zn^{2+}$
  Xu, Z.; Yoon, J.; Spring, D. R. *Chem. Soc. Rev.* **2010**, *39*, 1996 – 2006.
  Abstract:

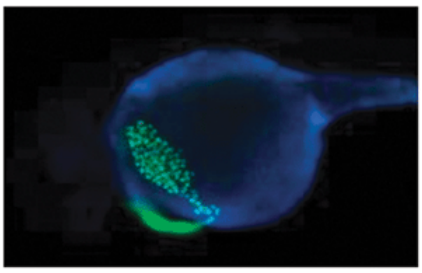

In the past decade, fluorescent chemosensors for zinc ion ($Zn^{2+}$) have attracted great attention because of the biological significance of zinc combined with the simplicity and high sensitivity of fluorescence assays. Chemosensors can be divided into a fluorophore, a spacer and a receptor unit; the receptor is the central processing unit (CPU) of a chemosensor. This *tutorial review* will classify zinc chemosensors based on receptor types.

- Conjugated Polymers That Respond to Oxidation with Increased Emission
  Dane, E. L.; King, S. B.; Swager, T. M. *J. Am. Chem. Soc.* **2010**, *132*, 7758–7768.
  Abstract:

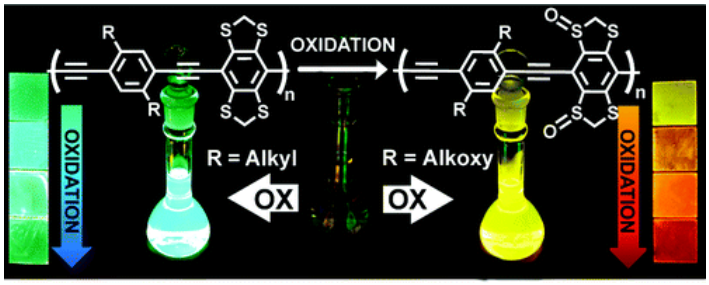


Thioether-containing poly(para-phenylene-ethynylene) (PPE) copolymers show a strong fluorescence turn-on response when exposed to oxidants in solution as a result of the selective conversion of thioether substituents into sulfoxides and sulfones. We propose that the increase in fluorescence quantum yield (ΦF) upon oxidation is the result of both an increase in the rate of fluorescence (kF), as a result of greater spatial overlap of the frontier molecular orbitals in the oxidized materials, and an increase in the fluorescence lifetime (τF), due to a decrease in the rate of nonradiative decay. Contrary to established literature, the reported sulfoxides do not always act as fluorescence quenchers. The oxidation is accompanied by spectral changes in the absorption and emission of the polymers, which are dramatic when oxidation causes the copolymer to acquire a donor–acceptor interaction. The oxidized polymers have high fluorescence quantum yields in the solid state, with some having increased photostability. A turn-on fluorescence response to hydrogen peroxide in organic solvents in the presence of an oxidation catalyst indicates the potential of thioether-containing materials for oxidant sensing. The reported polymers show promise as new materials in applications where photostability is important, where tunability of emission across the visible spectrum is desired, and where efficient emission is an advantage.

- Nanostructured Liquid Crystals Combining Ionic and Electronic Functions
  Yazaki, S.; Funahashi, M.; Kagimoto, J.; Ohno, H.; Kato, T. *J. Am. Chem. Soc.* **2010**, *132*, 7702–7708.

Abstract:

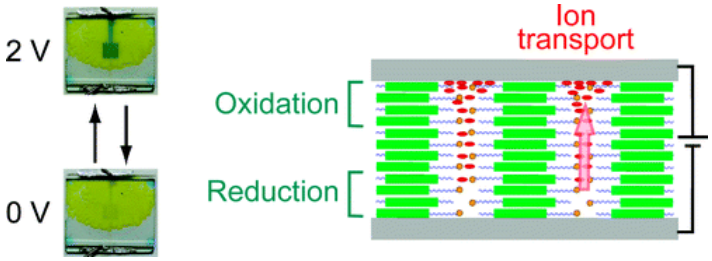


New molecular materials combining ionic and electronic functions have been prepared by using liquid crystals consisting of terthiophene-based mesogens and terminal imidazolium groups. These liquid crystals show thermotropic smectic A phases. Nanosegregation of the π-conjugated mesogens and the ionic imidazolium moieties leads to the formation of layered liquid-crystalline (LC) structures consisting of 2D alternating pathways for electronic charges and ionic species. These nanostructured materials act as efficient electrochromic redox systems that exhibit coupled electrochemical reduction and oxidation in the ordered bulk states. For example, compound 1 having the terthienylphenylcyanoethylene mesogen and the imidazolium triflate moiety forms the smectic LC nanostructure. Distinct reversible electrochromic responses are observed for compound 1 without additional electrolyte solution on the application of double-potential steps between 0 and 2.5 V in the smectic A phase at 160 °C. In contrast, compound 2 having a tetrafluorophenylterthiophene moiety and compound 3 having a phenylterthiophene moiety exhibit irreversible cathodic reduction and reversible anodic oxidation in the smectic A phases. The use of poly(3,4-ethylenedioxythiophene)−poly(4-styrene sulfonate) (PEDOT−PSS) as an electron-accepting layer on the cathode leads to the distinct electrochromic responses for 2 and 3. These results show that new self-organized molecular redox systems can be built by nanosegregated π-conjugated liquid crystals containing imidazolium moieties with and without electroactive thin layers on the electrodes.

- Direct Electrodeposition of Tetrahexahedral Pd Nanocrystals with High-Index Facets and High Catalytic Activity for Ethanol Electrooxidation
  Tian, N.; Zhou, Z.-Y.; Yu, N.-F.; Wang, L.-Y.; Sun, S.-G. *J. Am. Chem. Soc.* **2010**, *132*, 7580–7581.
  Abstract:

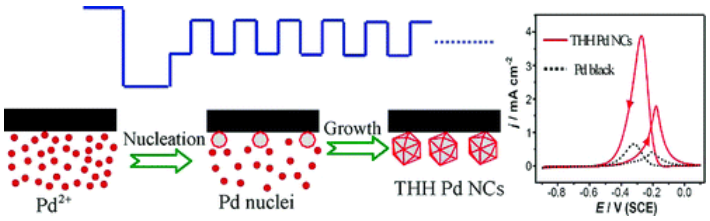


Tetrahexahedral Pd nanocrystals (THH Pd NCs) with {730} high-index facets were directly produced on a glassy carbon substrate in a dilute $PdCl_2$ solution by a newly developed programmed electrodeposition method. The THH Pd NCs, thanks to their high density of surface atomic steps, exhibit 4−6 times higher catalytic activity than commercial Pd black catalyst toward ethanol electrooxidation in alkaline solutions. This straightforward method provides a promising route to facile preparation of high-index-faceted metal nanocatalysts with high catalytic activity.

- Columnar Organization of Head-to-Tail Self-Assembled $Pt_4$ Rings

Frischmann, P. D.; Guieu, S.; Tabeshi, R.; MacLachlan, M. J. *J. Am. Chem. Soc.* **2010**, *132*, 7668–7675.

Abstract:

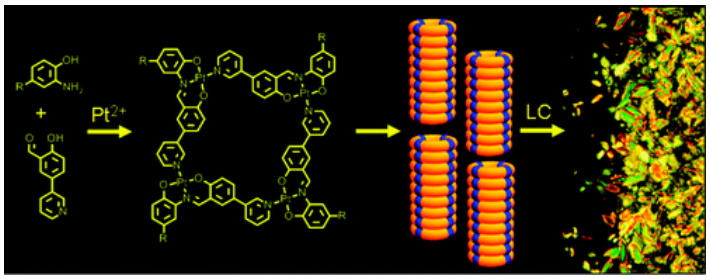


Coordination of $Pt^{2+}$ to a family of tunable Schiff base proligands directs the 12-component self-assembly of disk-shaped $Pt_4$ rings in a head-to-tail fashion. Aggregation of these $S_4$ symmetric $Pt_4$ macrocycles into columnar architectures was investigated by dynamic and static light scattering, NMR spectroscopy, powder X-ray diffraction, and transmission electron microscopy. Data from these experiments support the formation of columnar architectures for all of the structures studied except when bulky tris(4-*tert*-butylphenyl)methyl substituents were present. In this case, aggregation was limited to dimers in $CHCl_3$ ($K_{dim}$ = 3200 ± 200 L $mol^{-1}$ at 25 °C) and a thermodynamic analysis revealed that dimerization is an entropy driven process. Columnar architectures of $Pt_4$ rings with branched 2-hexyldecyl substituents organize into lyotropic mesophases in nonpolar organic solvents. These new self-assembled supramolecules are promising candidates to access nanotubes with multiple linear arrays of $Pt^{2+}$ ions.

- Molecular Conformation-Controlled Vesicle/Micelle Transition of Cationic Trimeric Surfactants in Aqueous Solution
  Wu, W.; Hou, Y.; Deng, M.; Huang, X.; Yu, D.; Xiang, J.; Liu, Y.; Li, Z.; Wang, Y. *Langmuir* **2010**, *26,* 7922–7927.
  Abstract:

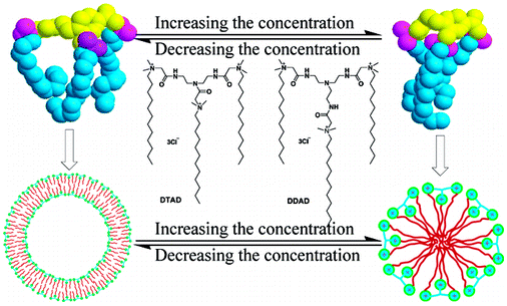


Two star-like trimeric cationic surfactants with amide groups in spacers, tri(dodecyldimethylammonioacetoxy)diethyltriamine trichloride (DTAD) and tri(dodecyldimethylammonioacetoxy)tris(2-aminoethyl)amine trichloride (DDAD), have been synthesized, and the aggregation behavior of the surfactants in aqueous solution has been investigated by surface tension, electrical conductivity, isothermal titration microcalorimetry, dynamic light scattering, cryogenic transmission electron microscopy, and NMR techniques. Typically, both the surfactants form vesicles just above critical aggregation concentration (CAC), and then the vesicles transfer to micelles gradually with an increase of the surfactant concentration. It is approved that the conformation of the surfactant molecules changes in this transition process. Just above the CAC, the hydrophobic chains of the surfactant molecules pack more loosely because of the rigid spacer and intramolecular electrostatic repulsion in the three-charged headgroup. With the increase

of the surfactant concentration, hydrophobic interaction becomes strong enough to pack the hydrophobic tails tightly and turn the molecular conformation into a pyramid-like shape, thus leading to the vesicle to micelle transition.

- Formation of Protein-Rich Coatings around Lipid Droplets Using the Electrostatic Deposition Method
  Cho, Y.-H.; Decker E. A.; McClements, D. J. *Langmuir* **2010**, *26*, 7937-7945.
  Abstract:

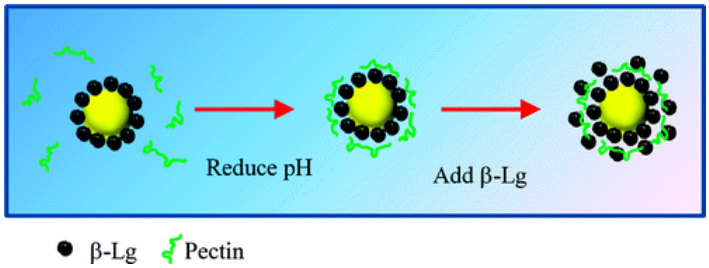


The purpose of this study was to determine whether protein-rich coatings could be formed around lipid droplets using an electrostatic deposition method. These coatings were assembled using two methods: (i) β-lactoglobulin was adsorbed to β-lactoglobulin-pectin-coated lipid droplets; (ii) β-lactoglobulin-pectin complexes were adsorbed to β-lactoglobulin-coated lipid droplets. Composite particles, consisting of lipid droplets with protein-rich biopolymer coatings, could be formed using both approaches (e.g., at pH 4, the protein surface load could be increased from 3 to 59 mg $m^{-2}$). These composite particles could be made small ($d$ < 500 nm) and relatively stable to gravitational separation at certain protein concentrations. Nevertheless, aggregation and sedimentation occurred at sufficiently high protein concentrations because of charge neutralization. The composite particles remained stable after they were heated above the thermal denaturation temperature of the globular proteins at pH 4. When the heated composite particles were adjusted to pH 7, where β-lactoglobulin and pectin are both negatively charged, some of the pectin and β-lactoglobulin became detached from the droplet surfaces but the protein surface load was still higher than in a nontreated sample. These composite particles may be useful for increasing the protein concentration in biopolymer coatings surrounding lipid droplets, which potentially has practical applications in the food industry (e.g., in protecting ω-3 oils from oxidation or in developing natural weighting agents.

- Total Synthesis of (-)-Dactylolide
  Yun, S. Y.; Hansen, E. C.; Volchkov, I.; Cho, E. J.; Lo, W. Y.; Lee, D. *Angew. Chem. Int. Ed*. **2010**, *49*, 4261 –4263.
  Abstract:

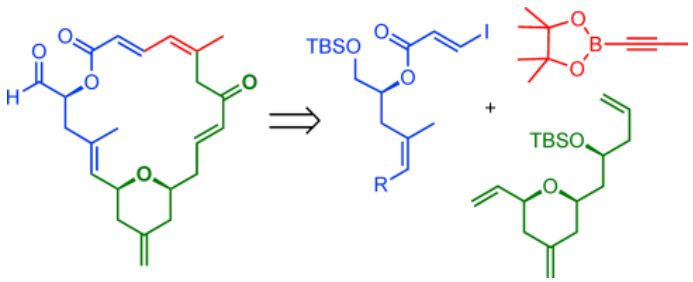


**Multiple metals in action**: Relying on the prowess of various metal-catalyzed C-O and C-C bond-forming reactions, a concise asymmetric total synthesis of (-)-dactylolide has been achieved (see scheme). The formation of a *Z*-trisubstituted vinylboronate through an Alder-ene reaction and

subsequent rhenium-mediated regioselective transposition of an allylic alcohol are the key features of this convergent synthesis.

- Self-Repair of a One-Dimensional Molecular Assembly in Mesoporous Silica by a Nanoscopic Template Effect
  Lintang, H. O.; Kinbara, K.; Tanaka, K.; Yamashita, T.; Aida, T. *Angew. Chem. Int. Ed.* **2010**, *49*, 4241 –4245.
  Abstract:

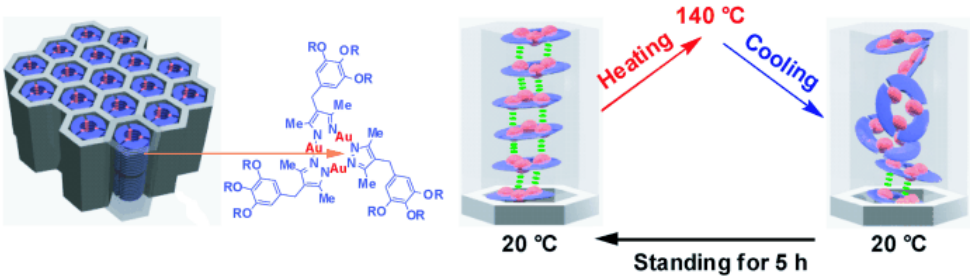


**Upon confinement** of a trinuclear gold(I) pyrazolate complex in a hexagonal silicate channel, the luminescence center formed by a $Au^{I}$-$Au^{I}$ metallophilic interaction is not only protected against thermal disruption but also strongly encouraged to self-recover from a heat-induced structural damage. This nanoscopic template effect is negligible for a lamellar silica framework.

- Tunable Optical Properties of Chromophores Derived from Oligo(*p*-phenylene vinylene)
  Guerlin, A.; Dumur, F.; Dumas, E.; Miomandre, F.; Wantz, G.; Mayer, C. R. *Org. Lett.* **2010**, *12*, 2382–2385.
  Abstract:

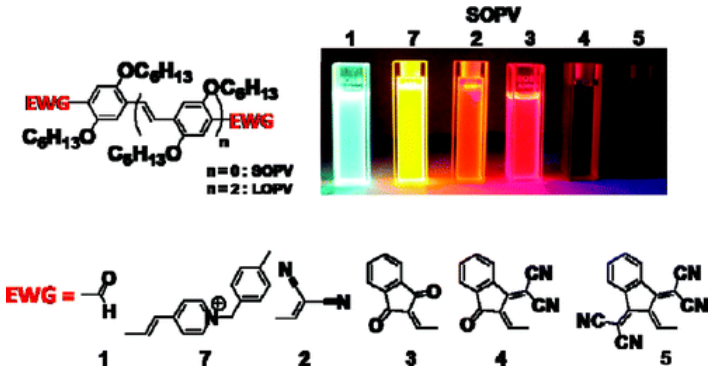


A series of 11 symmetric push−pull chromophores consisting of electron-accepting groups connected through a central π-conjugated system derived from oligo(*p*-phenylene vinylene) (OPV) were designed and synthesized. Electronic and spectroscopic properties were investigated by UV−visible absorption, fluorescence spectroscopy, and cyclic voltammetry. By finely tuning the electron-withdrawing ability of the acceptors as well as the length of the π-conjugated spacer, a wide range of dyes exhibiting strong absorption and emission were obtained.

- Increasing the Open Circuit Voltage of Bulk-Heterojunction Solar Cells by Raising the LUMO Level of the Acceptor
  Kooistra, F. B.; Knol, J.; Kastenberg, F.; Popescu, L. M.; Verhees, W. J. H.; Kroon, J. M.; Hummelen, J. C. *Org. Lett.* **2007**, *9*, 551–554.
  Abstract:

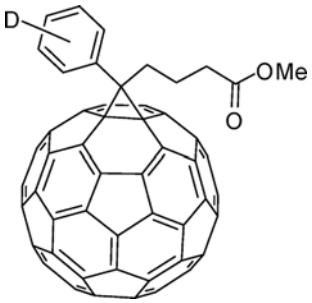


We report the synthesis, characterization, and electrochemical properties of ten new fullerene derivatives for usage in organic solar cells. The phenyl ring of PCBM was substituted with electron-donating and electron-withdrawing substituents to study their influence on the LUMO level of the parent fullerene. We varied the LUMO level over a range of 86 mV and show a small but significant change of the open circuit voltage upon application in MDMO−PPV:methanofullerene bulk-heterojunction photovoltaic cells.

- Peptide−Polymer Bioconjugates via Atom Transfer Radical Polymerization and Their Solution Aggregation into Hybrid Micro/Nanospheres for Dye Uptake
  Paira, T. K.; Banerjee, S.; Raula, M.; Kotal, A.; Si, S.; Mandal, T. K. *Macromolecules* **2010**, *43*, 4050–4061.
  Abstract:

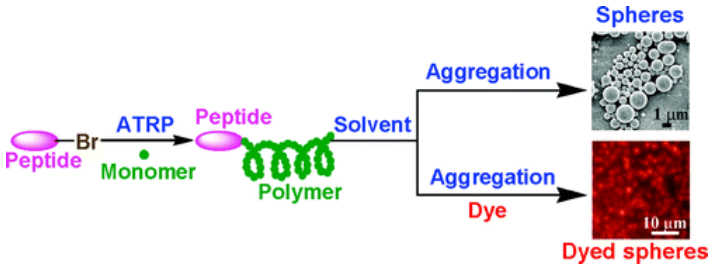


Peptide−polymer hybrid bioconjugates containing poly(methyl methacrylate) chains attached with oligopeptide molecules were prepared by atom transfer radical polymerization (ATRP) using designed peptide-initiators. These initiators were synthesized from newly designed peptides with 2-bromoisobutyric acid via a standard coupling reaction. ATRP of methyl methacrylate was conducted using Br-terminated peptide as macroinitiator and copper(I) chloride/*N*,*N*,*N*′,*N*″,*N*″-pentamethyldiethylenetriamine as the catalyst system in dimethyl sulfoxide (DMSO) at an elevated temperature (90 °C). The peptide−polymer bioconjugates with controllable molecular weights and low polydispersities (PDI < 1.35) were obtained. We devised a simple solution approach in assembling the peptide−polymer bioconjugate molecules into hybrid micro/nanospheres in different organic solvents as confirmed from transmission electron microscopy (TEM), field emission scanning electron microscopy (FESEM), and dynamic light scattering (DLS) results. The average size of the formed hybrid micro/nanospheres decreases with the increase of the polarity of the solvent used in aggregation process. A mechanistic model was suggested for the aggregation of peptide−polymer conjugates into hybrid micro/nanospheres that correlates well with the experimental observation. The dye-loaded hybrid micro/nanospheres were simply prepared by mixing an organic dye (Rhodamine 6G) into the aggregated solution of peptide−polymer bioconjugates. The uptake of dye into the micro/nanospheres was studied by fluorescence microscopy and time-correlated single photon counting (TCSPC) techniques.

- A Chemical Route to High Molecular Weight Vegetable Oil-Based Polyhydroxyalkanoate
  Petrovi, Z. S.; Mili, J.; Xu, Y.; Cvetkovi, I. *Macromolecules* **2010**, *43*, 4120–4125.
  Abstract:

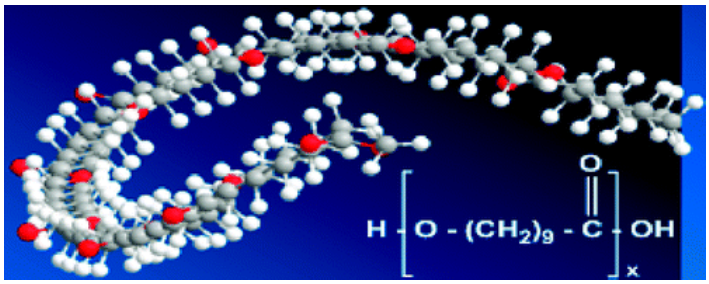


To our knowledge, this is the first description of the material properties of a high molecular weight linear polyester prepared from the methyl ester of 9-hydoxynonanoic acid (HNME). The HNME of high purity was prepared by ozonolysis of castor oil, followed by methanolysis of triglycerides. High molecular weight polyester prepared in bulk by transesterification was a highly crystalline material with limited solubility in chlorinated solvents. The polyester is an analogue of polycaprolactone (PCL), but the longer hydrocarbon chain between ester groups imparted intermediate properties between polyesters and polyethylene, characterized by a higher melting point, higher $T_g$, better thermal stability, and lower solubility in chlorinated solvents than PCL. Differential scanning calorimetry showed only a single transition-melting at 70 °C with melting enthalpy of 95 J/g. Properties of the material were strongly dependent on the molecular weight. Lower molecular weight material was brittle with low mechanical strength and higher crystallinity and melting point while the high molecular weight polymer was spinnable into fibers of high toughness, strength, and elongation. Dynamic mechanical analysis at 10 Hz revealed a glass transition at −38 °C, and dielectric analysis revealed behavior similar to PCL. The polymer was stable up to about 250 °C as observed by thermogravimetric analysis.

- Six-Component Reactions for the Stereoselective Synthesis of 3-Arylidene-2-oxindoles via Sequential One-Pot Ugi/Heck Carbocyclization/Sonogashira/Nucleophilic Addition
  Bararjanian, M.; Balalaie, S.; Rominger, F.; Movassagh, B.; Bijanzadeh, H. R. *J. Org. Chem.* **2010**, *75*, 2806–2812.
  Abstract:

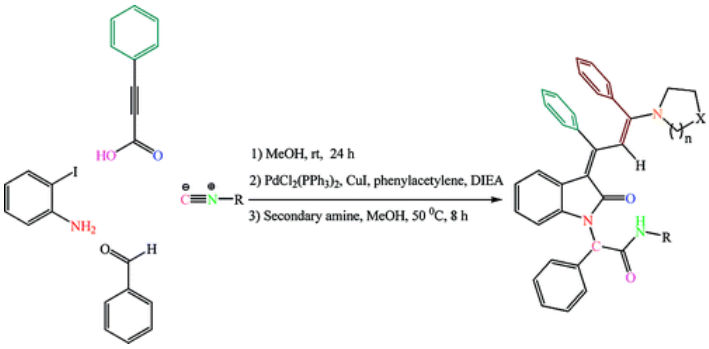


An efficient palladium-catalyzed protocol for the synthesis of 3-arylidene-2-oxindoles has been developed. In this approach, a sequential one-pot six-component reaction via Ugi/Heck carbocyclization/Sonogashira/nucleophilic addition was used for the synthesis of the desired skeleton.

- Copper-Mediated Cyclization–Halogenation and Cyclization–Cyanation Reactions of β-Hydroxyalkynes and *o*-Alkynylphenols and Anilines
  Swamy, N. K.; Yazici, A.; Pyne, S. G. *J. Org. Chem.* **2010**, *75*, 3412–3419.
  Abstract:

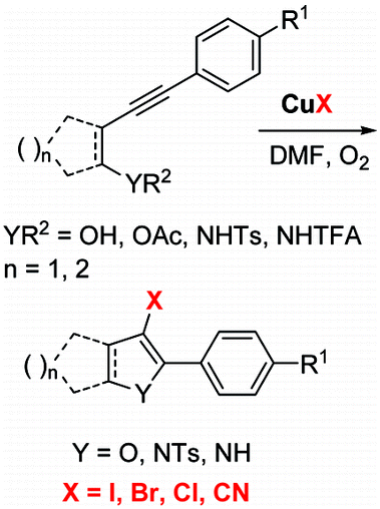


The CuX (X = I, Br, Cl, CN)-mediated cyclization–halogenation and cyclization–cyanation reactions of β-hydroxyalkynes and *o*-alkynylphenol and -aniline derivatives give rise to 3-halo- and 3-cyanofuro[3,2-*b*]pyrroles, 3-iodo-, 3-bromo-, and 3-cyanobenzofurans, and 3-cyanoindoles, respectively.

- Core-substituted naphthalenediimides
  Sakai, N.; Mareda, J.; Vauthey, E.; Matile, S. *Chem. Commun.* **2010**, *46*, 4225 – 4237.
  Abstract:

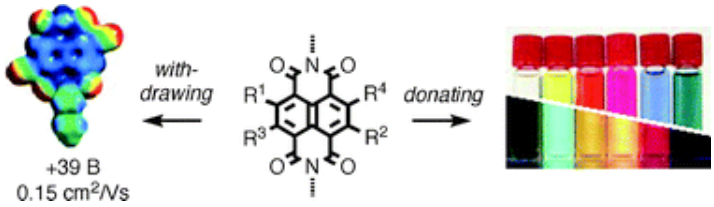


This feature article reviews research of core-substituted naphthalenediimides (cNDIs) in a comprehensive yet easily readable manner. Their synthesis, electrochemistry and spectroscopy are covered first with emphasis on the ability of cNDIs with electron donating substituents to absorb and fluoresce in all colors without global structural changes and cNDIs with electron withdrawing substituents to reach unprecedented extents of -acidity. The section on supramolecular chemistry covers face-to-face -stacks and peripheral hydrogen bonds, that on molecular recognition moves from pH and fluoride sensors to the binding to telomeric DNA in vivo and intercalation into -stacks and sticky tweezers. cNDIs can recognize and transport anions by functional anion– interactions. The section on electron transport describes cNDIs as air-stable n-semiconductors with high charge mobility and use as OFETs. Photoinduced electron transport by rainbow cNDIs has been used for the creation of artificial photosystems in solution, in bilayer membranes and on solid substrates. Examples include multicolor light harvesting architectures, organic solar cells, photosystems that can open up into ion channels, and supramolecular n/p-heterojunctions with antiparallel redox gradients. The review is highly interdisciplinary but should appeal most to organic, biosupramolecular and physical chemists.

- Supramolecular organization of extended benzobisoxazole cruciforms
  Osowska, K.; Miljani, O. *Chem. Commun.* **2010**, *46*, 4276 – 4278.
  Abstract:

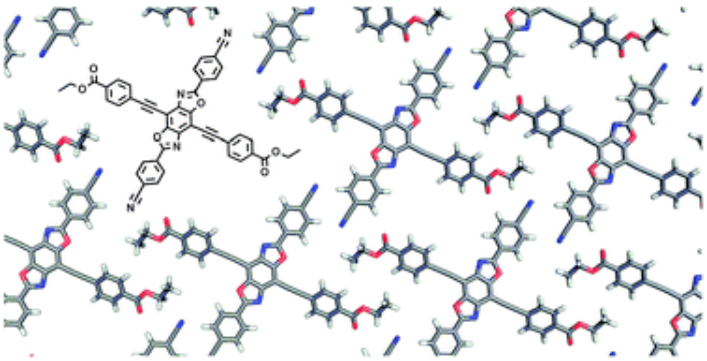

Extended benzobisoxazole-based cruciforms, efficiently synthesized using acyl condensations and Sonogashira couplings, form highly ordered two-dimensional sheets in the solid state.